Hydrodynamics of triangular-grid arrays of floating point-absorber wave energy converters with inter-body and bottom slack-mooring connections

Pedro C. Vicente[1], António F. de O. Falcão[1], Luís M.C. Gato[1], Paulo A.P. Justino[2]

[1]IDMEC, Instituto Superior Técnico, Technical University of Lisbon, 1049-001 Lisboa, Portugal

[2]Instituto Nacional de Engenharia, Tecnologia e Inovação, 1649-038 Lisboa, Portugal

E-mails: pedro.cabral.vicente@gmail.com; antonio.falcao@ist.utl.pt; luis.gato@ist.utl.pt; paulo.justino@ineti.pt

Abstract

It may be convenient that dense arrays of floating point absorbers are spread-moored to the sea bottom through only some of their elements (possibly located in the periphery), while the other array elements are prevented from drifting and colliding with each other by connections to adjacent elements. An array of identical floating point absorbers located at the grid points of an equilateral triangular grid is considered in the paper. A spread set of slack-mooring lines connect the peripheric floaters to the bottom. A weight is located at the centre of each triangle whose function is to pull the three floaters towards each other and keep the inter-body moorings lines under tension. The whole system – buoys, moorings and power take-off systems – is assumed linear, so that a frequency domain analysis may be employed. Equations are presented for a set of three identical point absorbers. This is then extended to more complex equilateral triangular grid arrays. Results from numerical simulations, with regular and irregular waves, are presented for the motions and power absorption of hemispherical converters in arrays of three and seven elements and different mooring and PTO parameters, and wave incidence angles. Comparisons are given with the unmoored and independently-moored buoy situations.

Keywords: Wave energy; Wave power; Arrays; Moorings; Point absorbers.

1 Introduction

Free floating devices are a large class of wave energy converters for deployment offshore, typically in water depths between 40 and 100m. As in the case of floating oil and gas platforms, such devices are subject to drift forces due to waves, currents and wind, and so they have to be kept on station by moorings (early contributions to the mooring design of wave energy converters can be found in [1,2]). Although similarities can be found between those applications, the mooring design requirements will have some important differences, one of them associated to the fact that, in the case of a wave energy converter, the mooring connections may significantly modify its energy absorption properties by interacting with its oscillations [3].

Among the wide variety of floating wave energy devices, point absorbers have been object of special development effort since the late 1970s. They are oscillating bodies whose horizontal dimensions are small in comparison with the representative wavelength. Examples of such devices, that have attained the stage of prototype tested in the sea, are the IPS buoy [4], Aquabuoy [5], Wavebob [6] and PowerBuoy [7]. Their rated power ranges typically from tens to hundreds of kW. The extensive exploitation of the offshore wave energy resource may require the deployment of dense arrays of absorbers, the distance between elements in the array being possibly tens of meters [8]. In such cases, it may be more convenient and economical that only (some) elements in the periphery of the array are directly slack-moored to the sea bottom, while the other elements of the array are prevented from drifting and colliding by connections to adjacent elements.

The mooring, especially the slack-mooring, of (individual) floating wave energy converters has been addressed in the last few years by several authors [3, 9-13]. Fitzgerald and Bergdahl [12] studied in detail the effect of the mooring connections upon the performance of a wave energy converter, by linearizing the mooring forces about the static condition, which conveniently allows a frequency-domain analysis to be applied. This technique is also adopted in the present paper.

Little attention seems to have been devoted in the published literature to the mooring design of free-floating point absorbers in dense arrays. This may be explained by the present stage of development of the technology (focusing on single prototypes) and/or by the restricted availability of such information.

Recently, Vicente et al. [14] addressed the array mooring problem in its simplest form by considering a set of two floating wave energy converters (WECs) aligned with the direction of propagation of the incoming waves. By linearizing the mooring and power take-off (PTO) forces, a frequency-domain analysis could be employed. This kind of modelling is adopted in the present paper for an array of three (rather than two) identical floating WECs in triangular configuration and for arbitrary wave incidence. Variations in mean surface level due to tides and drifting forces due to currents, waves and wind are ignored. The whole system – buoys, moorings and PTOs – is assumed linear, so that a frequency domain analysis may be employed. In the numerical simulations, three identical hemispherical buoys oscillate in heave, surge and sway, acted upon by the waves, the mooring system and their PTOs. The PTO consists of a linear damper whose force is proportional to the heave velocity. The hydrodynamic interference between bodies is ignored. Results from numerical simulations, with regular and irregular waves, are presented for the motions and power absorption of the converters, for different mooring and PTO parameters.

The governing equations of the triangular array can be used to build up a mathematical model for more complex arrays in which the floaters are located at the grid points of an equilateral triangular grid. Numerical results are shown for an array of seven buoys located at the vertices and the centre of a regular hexagon. The inter-buoy mooring system is provided by 18 lines and six weights, with a spread bottom-mooring system consisting of six lines.

Comparisons are given with the unmoored and independently moored buoy situations.

2. Governing equations for a three-buoy array

We consider three identical hemispherical buoys, 1, 2 and 3 in an equiangular triangular configuration, as shown in plan view in Fig. 1. The moorings consists of a spread system of three mooring lines 1, 2 and 3 connecting buoys 1, 2 and 3 to the sea bottom respectively, and three lines 1-4, 2-4 and 3-4 connecting the buoys to a centrally placed weight 4 (a body much denser than water) whose role is to pull the buoys towards the centre of the triangle. The inter-body mooring cables are assumed inelastic and of negligible mass. Since, in addition, we ignore damping (viscous) forces on these cables, they remain approximately rectilinear. All six lines are supposed to be attached to the centres of the bodies. In a plan view and in calm water, the centres of the buoys are located at the vertices of a triangle and the six connecting lines (three bottom-mooring lines and three inter-body mooring lines) are aligned with the bisectors of the triangle (Fig. 1).

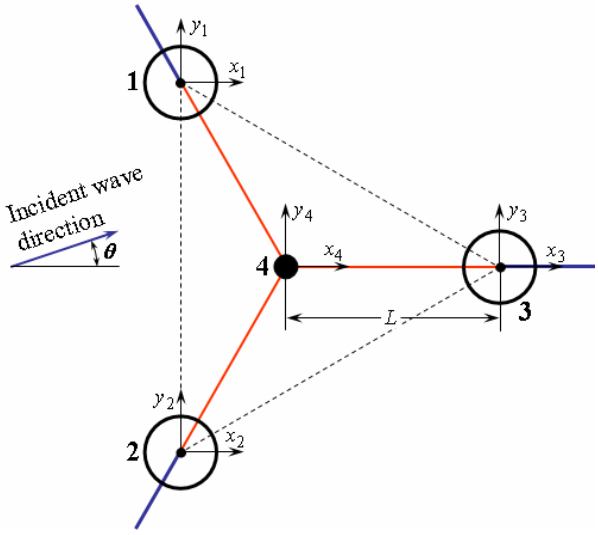

Fig. 1. Plan view of buoys 1 to 3, weight 4 and mooring lines in calm-sea static conditions. The wave direction makes an angle θ with the x-axes.

In the absence of waves, we assume that the centres of buoys lie on the free-surface plane, a distance L from the centre of the triangle and a distance $\sqrt{3}L$ apart from each other. Under calm sea conditions, the centre of body 4 is at distance $h=(G^2-L^2)^{1/2}$ below the free surface, where G is the length of cables 1-4, 2-4 and 3-4. The direction of propagation of the incident waves makes an angle θ with the x-axes, as shown in Fig. 1. The buoys and body 4, acted upon by the waves and mooring lines, are made to oscillate in heave and horizontally. Their centres are defined by coordinate systems (x_j, y_j, z_j) ($j=1$ to 4) (x_j and y_j are horizontal coordinates, and z_j is a vertical coordinate pointing upwards), with $x_j=y_j=z_j=0$ in the absence of waves (Fig. 1). The coordinates (x_4, y_4, z_4) of body 4 depend only on the instantaneous values of (x_j, y_j, z_j), $j=1$ to 3. We assume linear water wave theory to apply, which requires small wave-amplitude and small body motions. So it is reasonable to consider (x_j, y_j, z_j) as small compared with L and h. Neglecting products of small quantities, we find

$$x_4 - x_1 + \sqrt{3}(y_1 - y_4) + \frac{2h}{L}(z_1 - z_4) = 0, \qquad (1)$$

$$x_4 - x_2 - \sqrt{3}(y_2 - y_4) + \frac{2h}{L}(z_2 - z_4) = 0, \qquad (2)$$

$$x_4 - x_3 + \frac{h}{L}(z_4 - z_3) = 0. \qquad (3)$$

The pulling force vectors $\mathbf{F}_1$, $\mathbf{F}_2$ and $\mathbf{F}_3$ by the bottom-mooring lines make an angle β with the

horizontal plane which is assumed to be unchanged by the bodies' motions. The tension force vectors $\mathbf{R}_1$ (line 1-4), $\mathbf{R}_2$ (line 2-4) and $\mathbf{R}_3$ (line (3-4), and the corresponding angles α_1, α_2 and α_3 with the horizontal plane, depend on the instantaneous position of buoys 1, 2 and 3. In the absence of waves, it is $\alpha_1 = \alpha_2 = \alpha_3 = \alpha = \arctan(h/L) = \arccos(L/G)$, $F_1 = F_2 = F_3 = F$ and $R_1 = R_2 = R_3 = R$.

We easily find

$$R = (g/3)(m_4 - \rho v_4)\csc\alpha, \tag{4}$$

where g is the acceleration of gravity, ρ is water density, and m_4 and v_4 are the mass and volume of body 4 respectively. The bottom-mooring force F is related to R by

$$F = R\cos\alpha/\cos\beta. \tag{5}$$

We denote by f_j, r_j, ε_j ($j = 1$ to 3) the perturbations to the calm-sea values F, R, α. The values of (x_j, y_j, z_j) ($j = 1$ to 4) and f_j, r_j, ε_j ($j = 1$ to 3) are small quantities and this allows us to neglect their products. (Note: we assume the angle α to be neither small nor close to $\pi/2$.) We easily find, by neglecting small quantities of higher order,

$$\varepsilon_j = \frac{z_j - z_4}{G}\sec\alpha, \quad (j = 1, 2, 3). \tag{6}$$

The projections of lines 1-4, 2-4 and 3-4 on the horizontal plane make, with the x-direction, angles $\delta_1 - \pi/3$, $\delta_2 + \pi/3$ and $\delta_3 + \pi$, respectively. Here δ_j ($j = 1$ to 3) are small perturbation values, related to the bodies' coordinates by

$$\delta_1 = \frac{\sqrt{3}}{2L}(x_4 - x_1) + \frac{1}{2L}(y_4 - y_1), \tag{7}$$

$$\delta_2 = -\frac{\sqrt{3}}{2L}(x_4 - x_2) + \frac{1}{2L}(y_4 - y_2), \tag{8}$$

$$\delta_3 = \frac{1}{L}(y_3 - y_4). \tag{9}$$

Body 4 is subject to the pulling forces of lines 1-4, 2-4 and 3-4, its own weight gm_4, the buoyancy force $g\rho v_4$ and the hydrodynamic forces on it. By keeping only small quantities of first order, we find

$$\begin{aligned}(m_4 + A_{4h})\ddot{x}_4 + B_{4h}\dot{x}_4 - f_{d4h}\cos\theta \\ = R\frac{\sqrt{3}}{2}(\delta_2 - \delta_1)\cos\alpha + R\frac{\sin\alpha}{2}(\varepsilon_1 + \varepsilon_2) \\ - \frac{\cos\alpha}{2}(r_1 + r_2) - R\varepsilon_3\sin\alpha + r_3\cos\alpha,\end{aligned} \tag{10}$$

$$\begin{aligned}(m_4 + A_{4h})\ddot{y}_4 + B_{4h}\dot{y}_4 - f_{d4h}\sin\theta \\ = -R(\delta_1 + \delta_2)\frac{\cos\alpha}{2} + R\frac{\sqrt{3}}{2}(\varepsilon_2 - \varepsilon_1)\sin\alpha \\ + \frac{\sqrt{3}}{2}(r_1 - r_2)\cos\alpha + R\delta_3\cos\alpha,\end{aligned} \tag{11}$$

$$\begin{aligned}(m_4 + A_{4z})\ddot{z}_4 + B_{4z}\dot{z}_4 - f_{d4z} \\ = R(\varepsilon_1 + \varepsilon_2 + \varepsilon_3)\cos\alpha + (r_1 + r_2 + r_3)\sin\alpha.\end{aligned} \tag{12}$$

Here A_{4h}, A_{4z}, B_{4h}, B_{4z} are the hydrodynamic coefficients of added mass and radiation damping concerning the horizontal (subscript h) and heave (subscript z) oscillation modes of body 4, and f_{d4h} and f_{d4z} are the horizontal and vertical components of the wave excitation force on body 4 (see [15]).

Equations (1-3) and (7-12) yield r_j ($j = 1$ to 3) as linear functions of x_j, y_j, z_j ($j = 1$ to 3), of their time-derivatives and of the wave excitation force (f_{d4h}, f_{d4z}) on body 4.

A linearization procedure for the bottom-mooring forces has been explained in detail by Fitzgerald and Bergdahl [12], who showed that the linear approximation depends on the frequency and amplitude of the body motions and on the static condition of the cable.

We assume that the attachment angle β (with the horizontal plane) of the bottom-mooring cables 1, 2 and 3 remains unchanged Then, the extensions ϕ_j of mooring line j ($j = 1$ to 3) due to displacements (x_j, y_j, z_j) of the centre of body j are

$$\phi_1 = (x_1 - \sqrt{3}y_1)\frac{\cos\beta}{2} + z_1\sin\beta, \tag{13}$$

$$\phi_2 = (x_2 + \sqrt{3}y_2)\frac{\cos\beta}{2} + z_2\sin\beta, \tag{14}$$

$$\phi_3 = -x_3\cos\beta + z_3\sin\beta. \tag{15}$$

We now write, for the perturbation f_j to the mooring force F_j,

$$f_j = K\phi_j + D\dot{\phi}_j + \mu\ddot{\phi}_j \qquad (j = 1 \text{ to } 3), \tag{16}$$

where $K\phi_j$, $D\dot{\phi}_j$ and $\mu\ddot{\phi}_j$ are perturbation forces representing the spring effect, the linear damping and the inertia of the cable, respectively.

The PTO of each floating converter is assumed to consist of a simple linear damper activated by the buoy heaving motion. The vertical force it produces on the buoy is $-C\dot{z}_j$ ($j = 1$ to 3).

3. Frequency domain equations for a triangular array

Here, we neglect the hydrodynamic interference between the three bodies. Taking into account the spherical shape of the floaters, and recalling that the mooring lines are supposed to be attached to the centres of the bodies, it follows that the only significant modes of oscillation are heave, surge and sway, and also that these modes are hydrodynamically uncoupled

By following the usual linear decomposition of the hydrodynamics forces [15], we can now write the governing linear equations for the motions of floaters 1, 2 and 3

$$(m+A_h)\ddot{x}_1 + B_h\dot{x}_1 = r_1\frac{\cos\alpha}{2} + R\frac{\sqrt{3}}{2}\delta_1\cos\alpha - R\varepsilon_1\frac{\sin\alpha}{2} - f_1\frac{\cos\beta}{2} + f_{d1h}\cos\theta, \quad (17)$$

$$(m+A_h)\ddot{y}_1 + B_h\dot{y}_1 = -r_1\frac{\sqrt{3}}{2}\cos\alpha + R\delta_1\frac{\cos\alpha}{2} + R\frac{\sqrt{3}}{2}\varepsilon_1\sin\alpha + \frac{\sqrt{3}}{2}f_1\cos\beta + f_{d1h}\sin\theta, \quad (18)$$

$$(m+A_z)\ddot{z}_1 + (B_z+C)\dot{z}_1 + \rho g S z_1 = -R\varepsilon_1\cos\alpha - r_1\sin\alpha - f_1\sin\beta + f_{d1z}, \quad (19)$$

$$(m+A_h)\ddot{x}_2 + B_h\dot{x}_2 = r_2\frac{\cos\alpha}{2} - R\frac{\sqrt{3}}{2}\delta_2\cos\alpha - R\varepsilon_2\frac{\sin\alpha}{2} - f_1\frac{\cos\beta}{2} + f_{d2h}\cos\theta, \quad (20)$$

$$(m+A_h)\ddot{y}_2 + B_h\dot{y}_2 = r_2\frac{\sqrt{3}}{2}\cos\alpha + R\delta_2\frac{\cos\alpha}{2} - R\frac{\sqrt{3}}{2}\varepsilon_2\sin\alpha - \frac{\sqrt{3}}{2}f_2\cos\beta + f_{d2h}\sin\theta, \quad (21)$$

$$(m+A_z)\ddot{z}_2 + (B_z+C)\dot{z}_2 + \rho g S z_2 = -R\varepsilon_2\cos\alpha - r_2\sin\alpha - f_2\sin\beta + f_{d2z}, \quad (22)$$

$$(m+A_h)\ddot{x}_3 + B_h\dot{x}_3 = -r_3\cos\alpha + R\frac{\sqrt{3}}{2}\delta_3\cos\alpha + R\varepsilon_3\sin\alpha + f_3\cos\beta + f_{d3h}\cos\theta, \quad (23)$$

$$(m+A_h)\ddot{y}_3 + B_h\dot{y}_3 = -R\delta_3\cos\alpha + f_{d3h}\sin\theta, \quad (24)$$

$$(m+A_z)\ddot{z}_3 + (B_z+C)\dot{z}_3 + \rho g S z_3 = -R\varepsilon_3\cos\alpha - r_3\sin\alpha - f_3\sin\beta + f_{d3z}. \quad (25)$$

Here A_h, A_z and B_h, B_z are the hydrodynamic coefficients of added mass and radiation damping for the horizontal and vertical oscillations of the buoys, and f_{djh}, f_{djz} ($j=1$ to 3) are the horizontal and vertical components of the wave-induced excitation forces on buoys 1, 2 and 3. Besides, $S=\pi a^2$ is the cross-sectional area of the hemispherical floaters defined by the free surface plane in the absence of waves.

We recall that the perturbation angles ε_j, δ_j are linear functions of the coordinates of bodies 1, 2 and 3, and the perturbation forces r_j and f_j are linear functions of those coordinates and of their first and second time-derivatives.

Since Eqs (17-25) are linear, and assuming the incoming waves to be regular of angular frequency ω, we may write

$$\{x_j, y_j, z_j, f_{djh}, f_{djz}\} = \{X_j, Y_j, Z_j, \Phi_{jh}A_w, \Phi_{jz}A_w\}e^{i\omega t} \quad (j=1\text{ to }3), \quad (26)$$

where $X_j, Y_j, Z_j, \Phi_{jh}, \Phi_{jz}$ are (in general complex) amplitudes, and A_w is the incident wave amplitude. In Eq. (26), and whenever a physical quantity is equated to a complex expression, it is implicit that the real part is to be taken.

We easily find

$$\{\Phi_{jx}, \Phi_{jy}, \Phi_{jz}\} = \{\Phi_{3x}, \Phi_{3y}, \Phi_{3z}\}\chi_j \quad (j=1, 2), \quad (27)$$

where the complex factor

$$\chi_j = \exp(i\sqrt{3}kL\sin(\mp\theta+\pi/3)) \quad (28)$$

accounts for different phases due to different locations of the three buoys with respect to the incident wave crests. (In Eq. (28), the minus and plus signs are to be taken for $j=1$ and 2 respectively.)

If we now substitute from Eq. (26) for $x_j, y_j, z_j, f_{djh}, f_{djz}$ ($j=1$ to 3), we obtain, from Eqs. (17-25), a set of nine linear algebraic equations for the complex amplitudes X_j, Y_j, Z_j ($j=1$ to 3).

In regular waves, the time-averaged power absorbed by each floater is

$$\overline{P}_j = \frac{1}{2}C\omega^2|Z_j|^2 \quad (j=1\text{ to }3). \quad (29)$$

4. Numerical results for a three-buoy array

Deep water was assumed for the hydrodynamic coefficients of added mass, radiation damping and excitation force. Tabulated values (together with asymptotic expressions) can be found in [16] (in dimensionless form) for the added masses A_h, A_z and the radiation damping coefficients B_h, B_z of a floating hemisphere oscillating in heave and surge. The absolute value of the vertical excitation force coefficient may be obtained from $B_z(\omega)$ by using the Haskind relation (valid for an axisymmetric body oscillating in heave, see [7,17])

$$|\Phi_{jz}(\omega)| = \left\{\frac{2g^3\rho B_z(\omega)}{\omega^3}\right\}^{1/2} \quad (30)$$

($j=1$ to 3). Numerical values for $|\Phi_{jh}(\omega)|$ and for $\arg(\Phi_{jz}(\omega)/\Phi_{jh}(\omega))$ (not available from [16]) were obtained with the aid of the boundary element code WAMIT.

We set $\rho = 1025\,\mathrm{kg\,m^{-3}}$ (sea water density) and $g = 9.8\,\mathrm{m\,s^{-2}}$, and define dimensionless values, denoted by an asterisk, as $L^* = L/a$, $\{X_j^*, Y_j^*, Z_j^*\} = \{|X_j|, |Y_j|, |Z_j|\}/A_w$ ($j=1$ to 3),

$\omega^* = \omega(a/g)^{1/2}$, $C^* = C\rho^{-1}a^{-5/2}g^{-1/2}$ and $K^* = K/(\rho g S)$. Body 4 is a sphere of radius a_4 (dimensionless radius $a_4^* = a_4/a$) and density $\rho_4 = 2500\,\mathrm{kgm}^{-3}$ (typical of concrete). The submergence of body 4 is assumed to be sufficient for the excitation force and the radiation damping to be neglected, i.e. we set $B_{4h} = B_{4z} = 0$ and $f_{dAh} = f_{dAz} = 0$. For the added mass of body 4, we take the added mass of an accelerating sphere in an unbounded fluid (see e.g. [18]) $A_{4h} = A_{4z} = (2/3)\rho\pi a_4^3$. In all cases for which results are shown here it is $a_4^* = a_4/a = 0.2$, $L^* = L/a = 4$ and $\alpha = 30°$. Note that, since the buoy centre is assumed to lie on the free-surface horizontal plane in static conditions, the mass of the buoy slightly varies with the mooring parameters.

We recall that the hydrodynamic interference between the three buoys (due to the radiated and diffracted wave fields) is neglected, and so the interference between them is due solely to the presence of body 4 and the action of the inter-body mooring lines 1-4, 2-4 and 3-4.

In the numerical simulations, the viscous damping and inertia of the bottom-mooring cables are neglected, i.e. we set approximately $D = \mu = 0$.

4.1. Regular waves

The power performance of the three wave energy converters 1, 2 and 3 is defined by a dimensionless power absorption coefficient defined as $P_j^* = \overline{P}_j / \overline{P}_{\max}$ ($j = 1$ to 3), where $\overline{P}_{\max}$ is the theoretical maximum limit of the (time-averaged) power that an axisymmetric heaving wave energy converter can absorb from regular waves of frequency ω and amplitude A_w, and is known to be (see [15]) $\overline{P}_{\max} = g^3\rho A_w^2/(4\omega^3)$ (corresponding to capture width $\lambda/2\pi$).

Numerical results are presented in Figs 2 and 3, with wave angle of incidence $\theta = 0$. Comparisons are shown with a single buoy of the same size (with identical values of C, K and β as for the triple buoys), spread-moored by two lines (in the vertical plane of the incident wave direction) as well as unmoored.

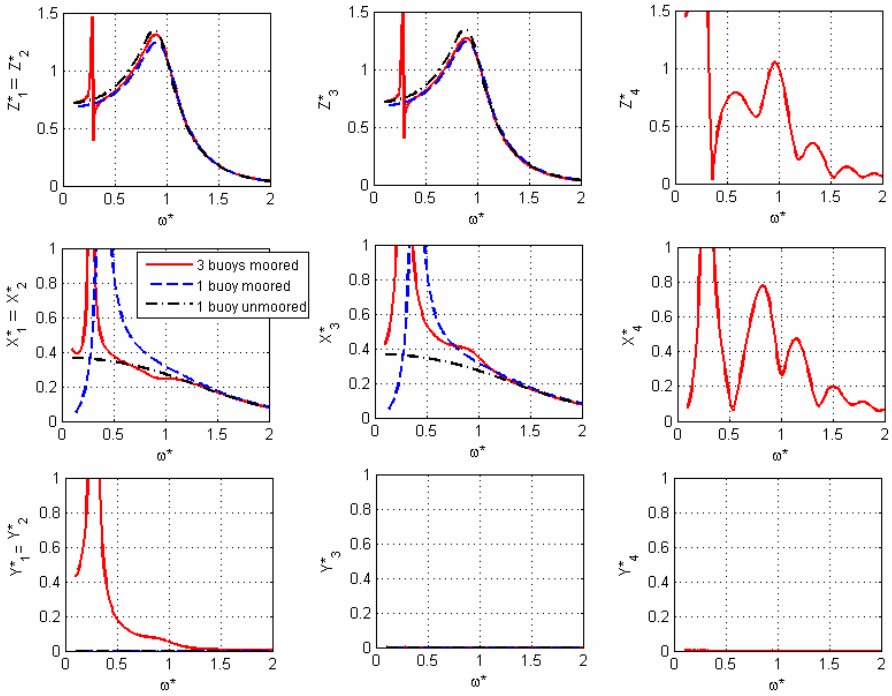

Fig. 2. Dimensionless oscillation amplitudes of buoys 1, 2 and 3 and body 4, compared with a moored and an unmoored single buoy of same size. Regular waves, with $\beta = 30°$, $\theta = 0$.

In the range of frequencies of practical interest, the amplitudes of heave oscillations of the moored buoys appear to be in general significantly larger compared with the surge oscillations. The heave oscillation amplitudes of the triple buoys are almost identical to those of the single moored buoy, and naturally are smaller than for the unmoored buoy. As compared with heave, the surge oscillations are significantly more sensitive to the mooring forces, especially in the lower wave frequencies (where resonance may occur). We note that the surge oscillations of buoys 1, 2 and 3, and the moored single buoy may be significantly different. Naturally, sway only occurs for the triple buoys due to the inter-body moorings forces.

Figure 2 shows that a resonance peak occurs at $\omega^* \cong 0.87$ for the heaving motion of the unmoored buoys, but not for the (uncoupled) surging mode (as expected, since no restoring force exists for the horizontal motions). In the cases of the moored buoys, the vertical component of the mooring forces is small compared with the hydrostatic restoring force (and so heaving resonance at about the same frequency also

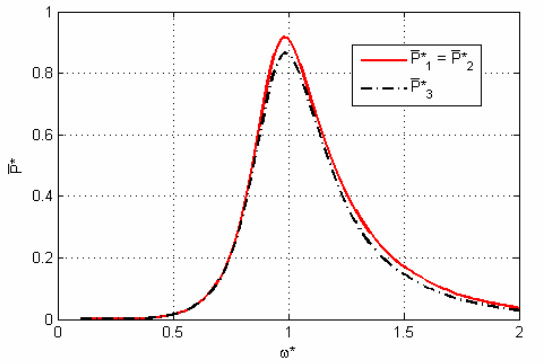

Fig. 3. Comparison of the dimensionless time-averaged power $\overline{P}^*$ absorbed by buoys 1, 2 and 3. Regular waves, with $\beta = 30°$, $\theta = 0$.

occurs). The situation is different for the surge mode. Here, the restoring force is small and due solely to the mooring lines, which explains the presence of a surge resonance peak at low frequencies: $\omega^* \cong 0.39$ for the individually moored buoy and $\omega^* \cong 0.28$ for the triple buoys. In the latter case, it may be seen that this induces a (very narrow) peak on the heaving motion. Close to these low-frequency resonances, the oscillation amplitudes are (unrealistically) large due to small radiation damping. The dimensionless contribution of these low-frequency peaks in terms of power appears negligible in Fig. 3. This may be explained by the fact that the PTO damping is set as $C^* = 0.362$ that maximizes the absorbed power by the unmoored buoy in resonance conditions. Anyway, the very narrow low-frequency peak apparent in the heaving mode turns out to have little effect in irregular waves (see the following subsection), firstly because of its narrowness and secondly because, in the power spectral distribution, it is located outside the range of significant energy content.

In the case of the triple moored buoys, the centre of gravity of the set, and also body 4, oscillate in heave but not horizontally, while, individually, buoys 1, 2 and 3 (apart from heaving) also perform horizontal oscillations while remaining (in planform) in equilateral triangular positioning.

Figure 3 (for $\theta = 0$) shows that buoys 1 and 2 extract more energy than buoy 3. It should be noted, as an explanation, that, although buoy 3 is subject to the same diffraction force as buoys 1 and 2 with a time delay, the same is not true for the inter-body mooring forces.

4.2. Irregular waves

Computations were also performed for one-directional irregular waves. A Pierson-Moskowitz spectral distribution was adopted, defined by (SI units, [19])

$$S(\omega) = 263\, H_s^2 T_e^{-4} \omega^{-5} \exp(-1054\, T_e^{-4} \omega^{-4}), \qquad (31)$$

where H_s is significant wave height and T_e is energy period. The time-averaged power output in irregular waves is

$$\overline{P}_{\mathrm{irr},j}(H_s, T_e) = 2\int_0^\infty \overline{P}_{1,j}(\omega)\, S(\omega)\, d\omega, \qquad (32)$$

where $\overline{P}_{1,j}(\omega)$ is the power absorbed by floater j from regular waves of frequency ω and unit amplitude. In dimensionless form, we write, for irregular waves, $P^*_{\mathrm{irr},j} = \overline{P}_{\mathrm{irr},j} \big/ \overline{P}_{\mathrm{max,irr}}$, where

$$\overline{P}_{\mathrm{max,irr}} = \frac{g^3 \rho}{2} \int_0^\infty \omega^{-3} S(\omega)\, d\omega = 149.5 H_s^2 T_e^3 \qquad (33)$$

(SI units) is the maximum (time-averaged) power that can be extracted by an axisymmetric body oscillating in heave in a sea state represented by the spectral distribution $S(\omega)$.

Time-series (for body displacements and velocities, instantaneous absorbed power, etc.) can be simulated by discretizing the spectral distribution (32) and superposing a large number N of regular waves of frequencies $\omega_n = \omega_0 + n\,\Delta\omega$, where $\Delta\omega$ is a small frequency interval, $n = 0, 1, 2, \ldots, N-1$, and the spectrum is supposed not to contain a significant amount of energy outside the frequency range $\omega_0 \le \omega \le \omega_0 + (N-1)\Delta\omega$. (In the numerical simulations, it was $\Delta\omega = 0.01$ rad/s, $\omega_0 = 0.05$ rad/s and $N = 200$.) The complex amplitude (at a fixed point) of the wave component of order n is $A_{w,n} = \left(2S(\omega_n)\Delta\omega\right)^{1/2} e^{i\phi_n}$. Here ϕ_n ($n = 0, 1, 2, \ldots, N-1$) are random real numbers in the interval $(0, 2\pi)$.

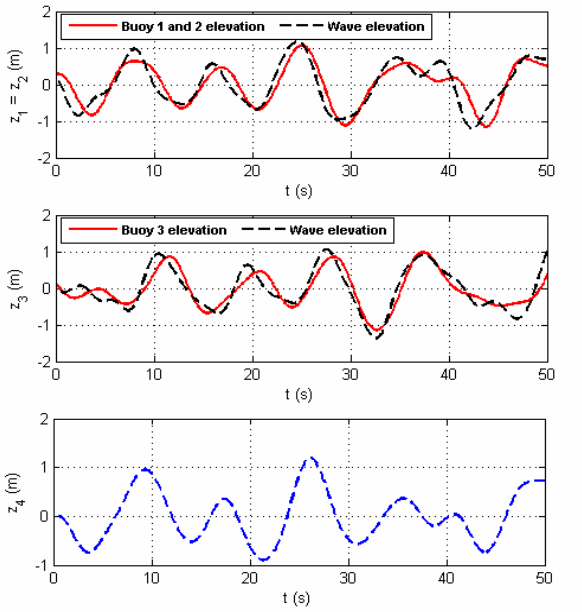

Fig. 4. Heave oscillations of buoys 1, 2 and 3 and body 4. Irregular waves of $H_s = 2$ m, $T_e = 10$ s, $\beta = 30°$, $\theta = 0$.

Numerical results are plotted in Figs. 4 and 5, for irregular waves of $H_s = 2$ m, $T_e = 10$ s, for $a = 7.5$ m,

$L = 30\,\mathrm{m}$, $\beta = 30°$, $\alpha = 30°$, $a_4^* = 0.2$, $K^* = 0.1$, $C^* = 0.315$.

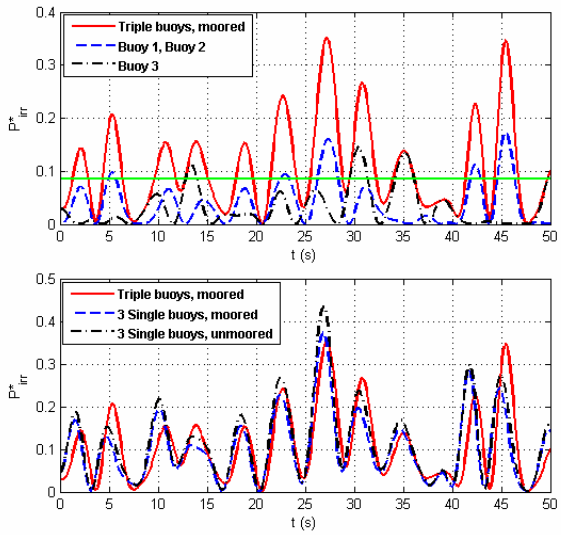

Fig. 5. On the top: Instantaneous dimensionless power P_{irr}^* absorbed by the triple buoys (red solid line) and by each buoy. On the bottom: Comparison between the power absorbed by the three-buoy array and by arrays of three unmoored buoys and three independently moored buoys. Irregular waves of $H_s = 2\,\mathrm{m}$, $T_e = 10\,\mathrm{s}$, $\beta = 30°$, $\theta = 0$

Figure 4 shows the heave oscillations for buoys 1 and 3, and for body 4. As should be expected, the time series for buoys 1 and 3 are not identical, due to their different locations and, to a less extent, to the cable interactions. Since it is $\theta = 0$, obviously the oscillations of buoy 1 and 2 are identical. The difference between the wave and the buoy elevations can be seen.

Figure 5 shows, on top, the time-varying power absorbed separately by buoy 1 (equal to that of buoy 2) and buoy 3, and the total power. The combination of three converters produces a smoothing effect on power, which would be even more effective in the case of an array with a larger number of elements, as can be seen in section 5 for a seven-buoy array. On the bottom of Fig. 5, a comparison is shown between the power absorbed by the triple buoy set and by an identical set in the unmoored and independently moored situations. The differences appear to be significant.

5. Complex triangular-grid arrays

The equations derived in sections 2 and 3 can be used without major difficulty to build up a mathematical model for more complex arrays consisting of buoys placed at the grid points of an equilateral triangular grid, with the weights located at the centres of the triangular cells. Each buoy is attached to a number of weights depending on the array and mooring configuration (see Fig. 6). As before, the instantaneous position in 3D-space of each weight depends only on the instantaneous position of the three buoys to which it is attached. The array is spread-moored to the sea bed through its peripheric buoys, in such way that, in calm water, the whole assembly conforms to the specified pattern.

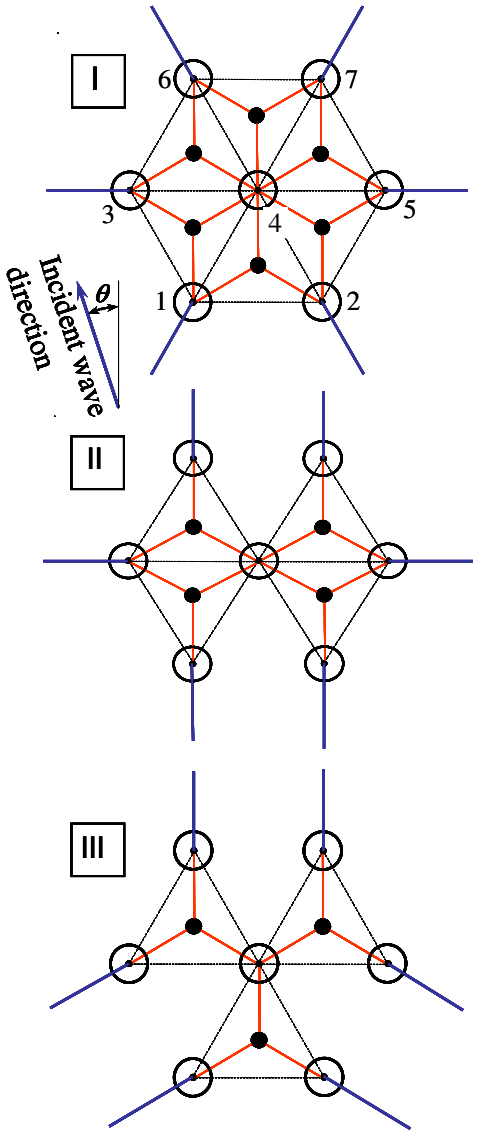

Fig. 6. Different mooring configurations, I, II and III, for a star array of seven point absorbers.

The numerical results in Figs 8-9 are for irregular waves of $H_s = 2\,\mathrm{m}$, $T_e = 10\,\mathrm{s}$, and for $a = 7.5\,\mathrm{m}$, $L = 30\,\mathrm{m}$, $\beta = 30°$, $\alpha = 30°$, $a_8^* = 0.2$ (dimensionless radius of the weights), $K^* = 0.1$, $C^* = 0.315$ and the angle of incidence is $\theta = 0$.

Figure 8 shows the heave, surge and sway oscillations for the seven buoys. Due to symmetry, the results are identical (of opposite sign for sway) for pairs of buoys 1-2, 3-5, 6-7, but not between different pairs due to different locations and to mooring effects.

Figure 9 shows the oscillations in the perturbation of the force F of the bottom moored buoys. It can be seen that configuration III is more demanding for the moorings.

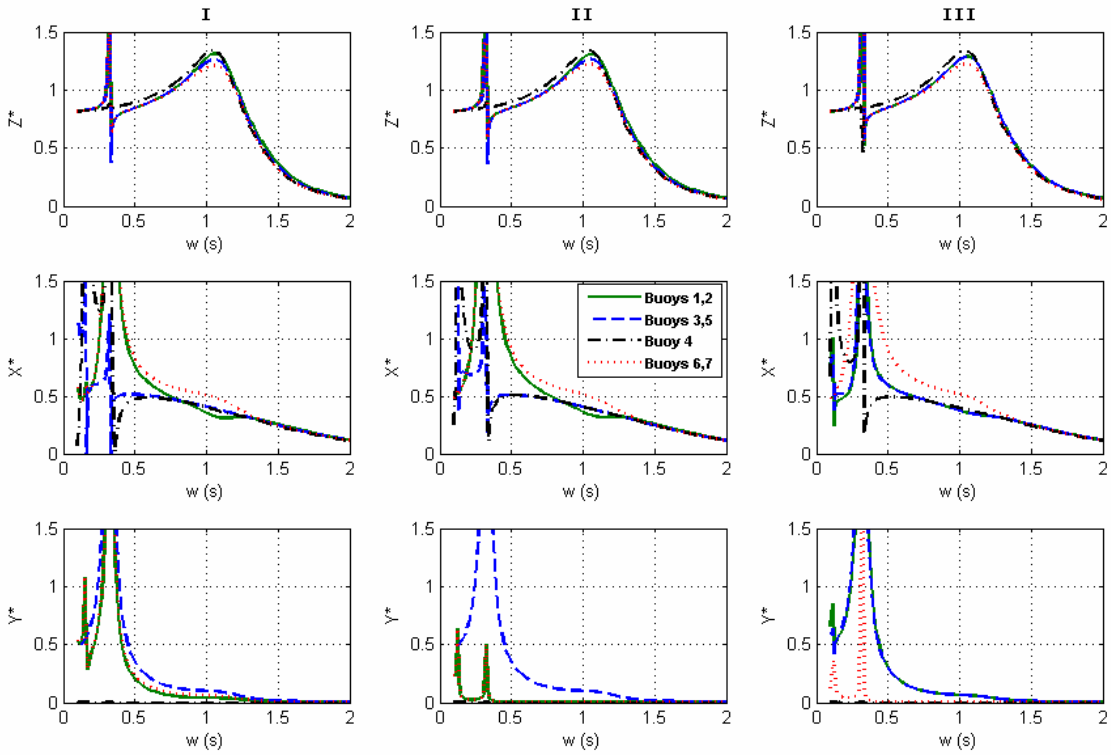

Fig. 7. Dimensionless oscillation amplitudes of the seven buoys for mooring configurations I, II and III for regular waves.

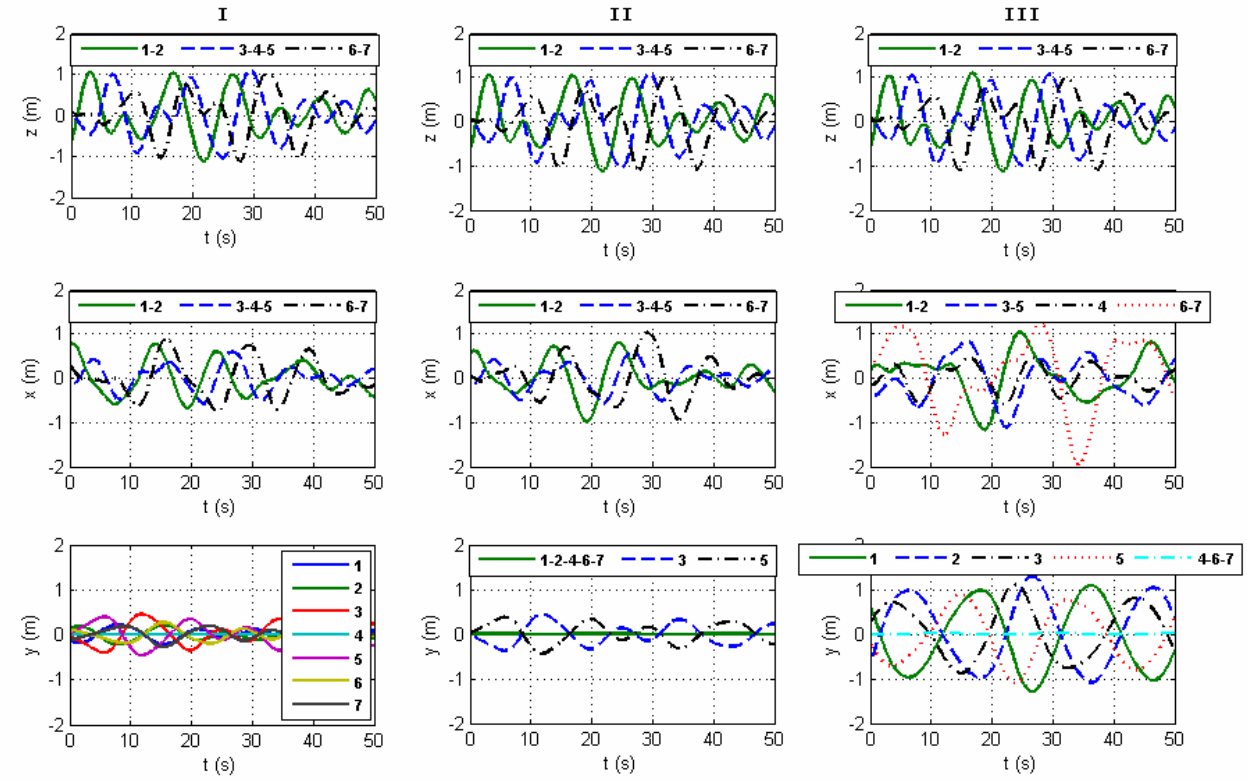

Fig. 8. Heave, surge and sway oscillations of the centres of the seven buoys for mooring configurations I, II and III. Irregular waves of $H_s = 2\text{m}$, $T_e = 10\text{s}$, $\beta = 30°$, $\theta = 0$.

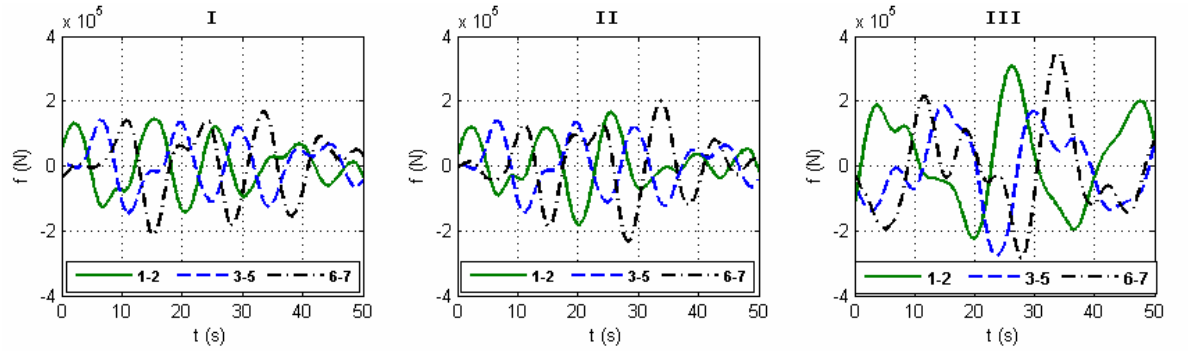

Fig. 9. Variation of the perturbations in the mooring force F for the bottom moored buoys in configurations I, II and III. Irregular waves of $H_s = 2\,\mathrm{m}$, $T_e = 10\,\mathrm{s}$, $\beta = 30°$, $\theta = 0$.

Conclusions

The results presented here illustrate the behaviour and power performance of triangular-grid arrays of identical wave energy converters, absorbing energy in the heaving mode from regular and irregular waves, spread-moored to the bottom through the bordering elements and inter-connected by lines kept under tension by weights. The performance was found to be significantly affected by the presence of the mooring system.

In the study of complex arrays, the choice of mooring arrangement was found to affect the surge and sway motions (and also the mooring forces) more than the heave oscillations.

Such effects should be superposed on the hydrodynamic interference (diffraction and radiation wave fields) between oscillating bodies which was not accounted for in this analysis. Mooring effects that are known to be significant were ignored in the numerical simulations, namely the catenary, damping and inertia effects of the mooring cables. Such effects require a more demanding time-domain analysis rather than a frequency-domain analysis.

Acknowledgement

The work reported here was partly supported by the Portuguese Foundation for Science and Technology (programme POCTI and contract No. PTDC/EME-MFE/66999/2006).

References

[1] McCormick, ME. 1981, Ocean Wave Energy Conversion," New York: Wiley. 1981.

[2] Fylling, IJ. Anchoring systems for wave energy converters. In: Proc 2nd Int Symp Wave Energy Utilization (H Berge, editor), Trondheim, Norway, 1982, pp. 229-251.

[3] Johanning, I, Smith, GH, Wolfram, J. Mooring design approach for wave energy converters. Proc Inst Mech Eng Part M-J Eng Marit Environ 2006; 220: 159-174.

[4] Cleason, L, Forsberg, J, Rylander, A, Sjöström, BO. Contribution to the theory and experience of energy production and transmission from the buoy-concept. In: Proc 2nd Int Symp Wave Energy Utilization, Trondheim, Norway, 1982, p. 345-370.

[5] Weinstein, A, Fredrikson, G, Parks, MJ, Nielsen, K. Aquabuoy, the offshore wave energy converter numerical modelling and optimization. In: Proc MTTS/IEEE Techno-Ocean '04 Conf, Kobe, Japan, 2004, vol. 4, p. 1854-1859.

[6] http://www.wavebob.com/

[7] http://www.oceanpowertechnologies.com/

[8] Ricci, P, Saulnier, J-B, Falcão, AF de O. Point-absorber arrays: a configuration study off the Portuguese west coast. In: Proc 7th European Wave Tidal Energy Conf, Porto, Portugal, 2007.

[9] Johanning, L, Smith, GH, Wolfram, J. Towards design standards for WEC moorings. In: Proc 6th European Wave Tidal Energy Conf, Glasgow, 2005.

[10] Johanning, L, Smith, GH, Wolfram, J. Interaction between mooring line damping and response frequency as a result of stiffness alterations in surge. In: Proc 25th Int Conf Offshore Mechanics Arctic Eng (OMAE 2006), Hamburg, 2006, Paper No. 2006-92373.

[11] Fitzgerald, J, Bergdahl, L. Considering mooring cables for offshore wave energy converters. In: Proc 7th European Wave Tidal Energy Conf, Porto, Portugal, 2007.

[12] Fitzgerald, J, Bergdahl, L. Including moorings in the assessment of a generic offshore energy converter: a frequency domain approach. Mar Struct 2008; 21: 23-46.

[13] Fonseca, N, Pascoal, R, Morais, T, Dias, R. Design of a mooring system with synthetic ropes for the FLOW wave energy converter. In: Proc 28th Int Conf Ocean Offshore Arctic Eng, Honolulu, Hawaii, 2009, Paper No. OMAE2009-80223.

[14] Vicente, PC, Falcão, AF de O, Gato, LMC, Justino, PAP. Hydrodynamics of multiple floating point-absorber wave energy systems with inter-body and bottom slack-mooring connections. In: Proc 28th Int Conf Ocean Offshore Arctic Eng, Honolulu, Hawaii, 2009, Paper No. OMAE2009-80245.

[15] Falnes, J. Ocean Waves and Oscillating Systems. Cambridge: Cambridge University Press, 2002.

[16] Hulme, A. The wave forces acting on a floating hemisphere undergoing forced periodic oscillations. J Fluid Mech 1982; **121**: 443-463.

[17] Newman, JN. The exciting forces on fixed bodies in waves. J Ship Res 1962; 6: 10-17.

[18] Lighthill, J. An Informal Introduction to Theoretical Fluid Mechanics. Oxford: Oxford University Press, 1986.

[19] Goda, Y. Random Seas and Design of Maritime Structures. 2nd edition, Singapore: World Scientific, 2000.